Developmental Cognitive Neuroscience 51 (2021) 100996

Contents lists available at ScienceDirect

Developmental Cognitive Neuroscience

journal homepage: www.elsevier.com/locate/dcn

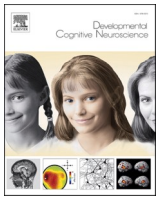

Effects of prenatal opioid exposure on functional networks in infancy

Stephanie L. Merhar [a,*,1], Weixiong Jiang [b,1], Nehal A. Parikh [a], Weiyan Yin [b], Zhen Zhou [b], Jean A. Tkach [c,d], Li Wang [b], Beth M. Kline-Fath [c,d], Lili He [a], Adebayo Braimah [c], Jennifer Vannest [e,1], Weili Lin [b,1]

[a] Perinatal Institute, Division of Neonatology, Cincinnati Children's Hospital and University of Cincinnati, Department of Pediatrics, Cincinnati, OH, USA
[b] Department of Radiology and BRIC, University of North Carolina at Chapel Hill, Chapel Hill, NC, USA
[c] Imaging Research Center, Cincinnati Children's Hospital, Cincinnati, OH, USA
[d] Department of Radiology, Cincinnati Children's Hospital, Cincinnati, OH, USA
[e] Department of Communication Sciences and Disorders, College of Allied Health Sciences, University of Cincinnati, Cincinnati, OH, USA

ARTICLE INFO

Keywords:
Neonatal
Opioid
Neonatal opioid withdrawal syndrome
Functional MRI
Functional connectivity
Magnetic resonance imaging

ABSTRACT

Prenatal opioid exposure has been linked to altered neurodevelopment and visual problems such as strabismus and nystagmus. The neural substrate underlying these alterations is unclear. Resting-state functional connectivity MRI (rsfMRI) is an advanced and well-established technique to evaluate brain networks. Few studies have examined the effects of prenatal opioid exposure on resting-state network connectivity in infancy. In this pilot study, we characterized network connectivity in opioid-exposed infants (n = 19) and controls (n = 20) between 4–8 weeks of age using both a whole-brain connectomic approach and a seed-based approach. Prenatal opioid exposure was associated with differences in distribution of betweenness centrality and connection length, with positive connections unique to each group significantly longer than common connections. The unique connections in the opioid-exposed group were more often inter-network connections while unique connections in controls and connections common to both groups were more often intra-network. The opioid-exposed group had smaller network volumes particularly in the primary visual network, but similar network strength as controls. Network topologies as determined by dice similarity index were different between groups, particularly in visual and executive control networks. These results may provide insight into the neural basis for the developmental and visual problems associated with prenatal opioid exposure.

1. Introduction

Opioid use during pregnancy remains high in the US, with one opioid-exposed infant born every 15 min (Honein et al., 2019). The effects of prenatal opioid exposure on the developing brain remain poorly understood. Multiple studies on outcomes in opioid-exposed children show adverse effects of maternal opioid use on neurodevelopment, behavior, and vision (Monnelly et al., 2019; Yeoh et al., 2019; Andersen et al., 2020; Arter et al., 2021; Nelson et al., 2020; Lee et al., 2020). In addition, animal studies show negative effects of maternal opioids on fetal oligodendrocytes and neurons. However, few human imaging studies have evaluated the effects of opioid exposure on the developing fetal brain.

In experimental animal models, prenatal exposure to opioids is associated with decreased neurotransmitter levels (Guo et al., 1990; Wu et al., 2001; Robinson et al., 1997), decreased neurogenesis (Wu et al., 2014; Erbs et al., 2016), increased apoptosis (Hu et al., 2002), and altered myelination (Vestal-Laborde et al., 2014; Sanchez et al., 2008). In addition, several studies in animal models (mostly rats and mice) show impaired learning and memory in the offspring of dams exposed to opioids during gestation (Chen et al., 2015; Van Wagoner et al., 1980; Zagon and McLaughlin, 1979; Alipio et al., 2020), In humans, multiple recent meta-analyses have examined the effects of prenatal opioid exposure on neurodevelopment and behavior (Monnelly et al., 2019; Yeoh et al., 2019; Andersen et al., 2020; Arter et al., 2021; Nelson et al., 2020; Lee et al., 2020). All found that opioid-exposed infants and children performed more poorly than non-exposed children across all domains examined, including cognition, motor development, behavior,

* Corresponding author at: Perinatal Institute, Cincinnati Children's Hospital, 3333 Burnet Ave ML 7009, Cincinnati, OH, 45229, USA.
E-mail address: stephanie.merhar@cchmc.org (S.L. Merhar).
[1] These authors contributed equally.

https://doi.org/10.1016/j.dcn.2021.100996
Received 30 January 2021; Received in revised form 22 July 2021; Accepted 29 July 2021
Available online 31 July 2021

attention, and vision. Most of these meta-analyses commented that the results may be biased, with many studies unable to control for additional risk factors for poor outcome in the opioid-exposed group.

Neonatal imaging studies suggest that prenatal opioid exposure may affect the structure and microstructure of the developing brain. In particular, infants prenatally exposed to methadone show decreased fractional anisotropy on diffusion tensor imaging in the first weeks of life compared with unexposed infants (Monnelly et al., 2018). Infants exposed to opioids prenatally show decreased brain volumes in multiple regions compared to unexposed infants (Merhar et al., 2020).

Resting-state functional MRI (rsfMRI) is a powerful technique that can be used to gain insight into the brain's functional organization during infancy. Studies have consistently shown that functional networks in the brain are present at birth and mature over the first years of life (Gao et al., 2015), and small-world network topology is also present at birth and becomes more efficient over the first 2 years (Gao et al., 2011; Jiang et al., 2019a). Normal development of brain networks and topology is known to be altered by prenatal drug (Grewen et al., 2015; Salzwedel et al., 2015) and alcohol (Roos et al., 2021) exposure. To our knowledge, only one small study has evaluated the functional connectivity of the brain in opioid-exposed infants, focusing on the amygdala (Radhakrishnan et al., 2021). The study found increased functional connectivity from the amygdala to several cortical areas in exposed infants compared to controls.

The aim of our pilot study in infants 4–8 weeks of age was to examine functional connectivity using rsfMRI in infants exposed to opioids prenatally and unexposed controls. We aimed to characterize network-specific differences between the two groups using a whole-brain connectomic approach. In addition, we focused on a specific set of functional networks known to underlie particular sensory and cognitive functions and examined connectivity with these networks as seeds. Previous studies on prenatal substance exposure have consistently shown functional hyperconnectivity in exposed groups compared with controls within pre-selected brain regions and/or networks (Salzwedel et al., 2015; Radhakrishnan et al., 2021; Salzwedel et al., 2016). Given these previous results and the consistent effects of prenatal opioid exposure on development, behavior, and sensory functions (vision in particular), we extended this area of research by further evaluating how opioid exposure may impact brain functional development at both the whole brain and network levels and hypothesized that opioid-exposed infants would show unique functional connectivity features when compared to control infants in visual and higher order networks.

2. Materials and methods

2.1. Participants

Infants born at ≥37 weeks gestation with prenatal opioid exposure and no other medical problems were recruited from clinics at Cincinnati Children's Hospital or from birth hospitals in the Greater Cincinnati area. Healthy control infants born at ≥37 weeks gestation were recruited from birth hospitals, from the Pediatric Primary Care clinic at Cincinnati Children's, or through community research advertisements. Infants in both groups were excluded if they had known chromosomal disorders or congenital anomalies, required any positive pressure ventilation outside of the delivery room, or had any conditions besides neonatal opioid withdrawal syndrome that required a NICU stay. Prenatal opioid exposure was determined by maternal history and/or maternal urine toxicology screen at the time of delivery and confirmed with neonatal toxicology screen (meconium or umbilical cord). All infants in the opioid-exposed group had exposure to opioids throughout pregnancy, but detailed information about the opioid(s) infants were exposed to during each week of pregnancy was not available. Lack of opioid or other drug exposure in controls was confirmed by maternal history and maternal urine toxicology screen at the time of delivery, which is standard clinical practice in our region. Additional information about drug exposure was collected by review of infant medical records and by maternal questionnaire at the time of MRI. Pregnancy and birth history were collected by review of infant medical records. Information about maternal socioeconomic status (including education, employment, and income) and race was collected by maternal questionnaire at the time of MRI. This study was approved by the Institutional Review Boards at Cincinnati Children's Hospital, Good Samaritan Hospital, and St. Elizabeth Hospital. Written informed consent was obtained from a parent or guardian prior to any study procedures.

2.2. MRI imaging acquisition

Infants were scanned during sleep with no sedation. All infants had been weaned off medications for neonatal opioid withdrawal syndrome by the time of scan. Infants were fed, swaddled, fitted with ear protection, placed in the Med-Vac vacuum bag (CFI Medical Solutions, Fenton MI), and moved into the scanner bore. All infants were scanned on the same Philips 3 T Ingenia scanner with 32 channel receive head coil in the Imaging Research Center at Cincinnati Children's Hospital. Structural MR imaging included a sagittal magnetization prepared inversion recovery 3D T1-weighted gradient echo sequence (shot interval = 2300 milliseconds, repetition time = 7.6 milliseconds, echo time = 3.6 milliseconds, inversion time = 1100 milliseconds, flip angle = 11 degrees, voxel size 1 mm x 1 mm x 1 mm, acceleration (SENSE) = 1 in plane and 2.0 through plane (slice) phase encode, scan time 3 min 6 s) and an axial 2D T2-weighted fast spin echo sequence (repetition time = 19100–19500 milliseconds, echo time = 166 milliseconds, voxel size 1 mm × 1 mm × 1 mm, acceleration (SENSE) = 1.5 in plane phase encode, scan time 3 min 50 s). Resting state functional MRI was obtained using an axial gradient echo echo-planar imaging sequence with simultaneous multi-slice excitation (multi-band) (repetition time = 1011 ms, echo time = 45 ms, flip angle = 54 degrees, voxel size 2.25 mm × 2.25 mm × 2.25 mm, 60 contiguous slices, multi-band factor = 6, 500 dynamics, scan time 8 min 37 s). Structural images were reviewed by a board-certified pediatric neuroradiologist to confirm there were no significant clinically relevant abnormalities (BK).

2.3. Statistical analysis of demographic/clinical data

This analysis was performed in STATA 16.0 (Stata Corp., College Station, TX). Descriptive statistics for the two groups (opioid-exposed and controls) were computed. Groups were compared using two-sided t-tests for continuous variables and Fisher's exact test for categorical variables, with a p-value of <0.05 considered significant for demographic variables.

2.4. MRI processing

2.4.1. Pre-processing

MRI data were pre-processed using an in-house infant-specific pipeline (Wu et al., 2012; Wang et al., 2015; Jiang et al., 2019b) which shares some common steps with the HCP pipeline (https://github.com/Washington-University/Pipelines), including head motion correction, alignment of rsfMRI images to T1 space, and band-pass filtering (0.01 Hz-0.08 Hz), but adds several unique steps tailored to infant functional connectivity MRI (Kam et al., 2019). Brain tissue segmentation was first conducted to generate tissue labeling maps (gray matter, white matter, or cerebrospinal fluid) using a multi-site infant-dedicated computational toolbox, iBEAT v2.0 Cloud (http://www.ibeat.cloud) (Wang et al., 2018). The tissue labeling maps were used to register to the template (Colin 27 atlas) (Holmes et al., 1998) in MNI space using advanced normalization tools (ANTs) (Avants et al., 2011). Automatic noise-related component detection and regression were performed (Kam et al., 2019). Specifically, a deep learning-based rsfMRI QC method, the long short-term memory (LSTM) neural network (Yan et al., 2018, 2019), was employed, capable of effectively extracting FC

quality-related features from the raw data. The deep learning-based approach considered not only head motion indices that have been widely used, but also several other important parameters, including the signal-to-noise of the raw images, temporal signal-to-noise ratio (tSNR) as well as grey-scale differences between neighboring volumes (Badhwar et al., 2020; Van Dijk et al., 2012). Specifically, the LSTM neural network method for deep time-series learning was implemented, aiming to yield three classes of image quality: passed, questionable, or failed. To achieve this goal, we adopted a two-stage strategy. We first engineered eight diagnostic features (maximum grey-scale difference between neighboring volumes of raw data, tSNR of raw fMRI data, maximum translation and rotation along all directions, mean framewise displacement (FD), percentage of number of the time points with large FD > 0.5 mm, quality of FC in primary visual and sensorimotor network) at different processing stages to generate initial QC labels, including passed, failed and questionable. Subsequently, we leveraged semi-supervised learning LSTM-based QC model to further examine the data that were deemed questionable and reassigned these data to either passed or failed. All preprocessing steps, including resampling and denoising, were conducted in each subject's native space.

2.4.2. Connectome-based analysis

The preprocessed functional data was parcellated into 90 regions of interest (ROIs) encompassing both cortical and subcortical areas in the AAL atlas (Tzourio-Mazoyer et al., 2002). First, the atlas in the standard Montreal Neurological Institute (MNI) space was warped to each subject's native space to extract regional averaged time series for post-processing. Pairwise functional connections were then calculated in the original space and Fisher z-transformed. Positive connections that differed significantly from zero were identified separately for the opioid-exposed and control groups ($p < 0.05$, corrected for multiple comparisons via false discovery rate (FDR)). We focused on positive connections for this analysis given the controversy in the literature about the meaning of negative connections (Weissenbacher et al., 2009; Hutchison et al., 2013; Garrison et al., 2015) although we have included information about negative connections in the supporting materials. The identified significant connections were further separated into three groups: the connections that overlapped between the two groups as well as unique functional connections in each group.

To better characterize the network architecture present in the opioid-exposed and control groups, we chose to focus on the graph theory metric *betweenness centrality* as a primary method to determine which regions played the most central role in opioid-exposed and control groups separately. Betweenness centrality refers to the fraction of all shortest paths in a network that pass through a given node, thus identifying the most central nodes in a network (Rubinov and Sporns, 2010). We also calculated normalized rich-club coefficients for each subject. The rich-club coefficient is a quantitative measure to discern the presence or absence of rich-club topology. We next examined the anatomic length of unique connections in each group and those that overlapped, using their anatomical coordinates in MNI space ($\sqrt{\Delta x^2 + \Delta y^2 + \Delta z^2}$). Finally, we examined how many of the unique and overlapping connections were components of particular known functional networks; specifically, the visual, default mode (DMN), sensorimotor, auditory, and attention networks using the network parcellation proposed by Tao et al. Tao et al. (2013).

2.4.3. Seed-based analysis

To further assess if prenatal opioid exposure impacts brain functional networks, a seed-based approach was employed. Eight networks using the regions reported by Smith et al. Smith et al. (2009) were used as seeds: V1 (medial visual), V2 (occipital pole), V3 (lateral visual), DMN (default mode network), SM (sensorimotor), AN (auditory), SA (executive control/salience), and FPN (bilateral frontoparietal). First, we transformed each seed into individual original space, then extracted the time series of each seed based on the preprocessed data with spatial smoothing using a 4 mm full-width half-maximum kernel. AFNI software (https://afni.nimh.nih.gov) was used for all seed-based calculations. The connectivity map of each seed was generated in subject space and then transformed to MNI space for subsequent statistical comparison and modeling. Regions of significant functional connectivity within a given seed network in each group were calculated on a voxel-wise basis ($p < 0.05$, FDR corrected, minimum cluster size: 50). Using the resulting mask of regions of significant functional connectivity, we calculated the cluster volume (number of voxels) and mean connectivity strength (r) for each seed network for each group, as well as the dice similarity index, which measures the spatial similarity between two sets of topologies. A dice index of >0.7 indicates that networks have similar topologies (Zijdenbos et al., 1994; Juneja et al., 2013).

3. Results

Demographic data is shown in Table 1. The groups had similar sex and age distributions. Of a total sample of 49 infants (21 opioid-exposed and 28 controls) with completed MRIs, 10 infants were excluded due to excessive motion or poor data quality, leaving a final sample of 19 opioid-exposed and 20 control infants for analysis. Of the 10 excluded infants, six subjects had less than 250 time points after removing time points that did not pass QC and four subjects had incomplete brain coverage. We compared the numbers of time points that were removed between the opioid-exposed (433.70 ± 70.55) and control (427 ± 81.62) groups using a *t*-test and no significant differences were observed ($p = 0.7634$). On review by a pediatric neuroradiologist, no infant in either group had overt brain injury. Two infants in the opioid-exposed group and two infants in the control group had incidental findings of small cerebellar hemorrhages. Three infants in the opioid-exposed group each had a single punctate periventricular white matter lesion. Information about neonatal opioid withdrawal syndrome for the 19 opioid-exposed infants is provided in Table 2.

3.1. Connectome-based analysis

We found 121 significant positive connections unique to the opioid-

Table 1
Demographics of study population.

	Opioid-exposed (n = 19)	Controls (n = 20)	p value
Male, n (%)	6 (32 %)	8 (40 %)	0.74
Gestational age at birth (weeks), mean (SD)	38.6 (0.8)	38.9 (0.8)	0.24
Birth weight (g), mean (SD)	3049 (261)	3323 (340)	0.008
Head circumference at birth (cm), mean (SD)	34.0 (1.2)	34.0 (1.5)	0.97
Postmenstrual age at scan (weeks), mean (SD)	44.5 (1.3)	45.2 (1.5)	0.12
Race/ethnicity			0.29
Non-Hispanic White	14	10	
Non-Hispanic Black	4	7	
Hispanic White	1	3	
Maternal smoking, n (%)	18 (94 %)	1 (4 %)	<0.001
Any maternal alcohol use during pregnancy	1 (5 %)	1 (4 %)	1.0
Maternal Hepatitis C, n (%)	12 (63 %)	0 (0 %)	<0.001
Maternal college degree, n (%)	4 (21 %)	16 (80 %)	<0.001
Maternal methadone, n (%)	6 (32 %)	n/a	n/a
Maternal buprenorphine, n (%)	12 (63 %)	n/a	n/a
Maternal heroin and/or fentanyl, n (%)	8 (42 %)	n/a	n/a
Other maternal illicit drug use	5 (26 %)	n/a	n/a
Neonatal abstinence syndrome requiring opioid treatment, n (%)	6 (32 %)	n/a	n/a

Two-sided *t*-test was used to compare continuous variables and Fisher's exact test was used to compare categorical variables.

Table 2
Information about neonatal opioid withdrawal syndrome symptoms and treatment.

Subject number	Postnatal opioid treatment for NOWS	Days of postnatal opioid exposure	Secondary medications for NOWS	Highest Finnegan score	Average Finnegan score on day of life 3
1	methadone	9		16	8
2	buprenorphine	6		13	7.6
3				17	7.9
4	methadone	10		12	8
5	buprenorphine	10	phenobarbital	15	9.8
6				12	9.3
7				4	3
8				8	1.6
9				13	7.4
10	buprenorphine	14		16	7.6
11				6	3
12				13	2.5
13	buprenorphine	6	clonidine	17	5.3
14				10	5.3
15				2	0.25
16				2	0.25
17				7	1.9
18				10	6.4
19				13	8.5

exposed group, 135 significant positive connections unique to the control group, and 459 positive connections that were common between the two groups. We compared the connection length among these connections. The connections unique to the opioid-exposed group as well as the connections unique to the control group were longer than those that overlapped between groups, which tended to be shorter ($t(37) = 8.63$, $t(37) = 9.88$, respectively, both $p < 0.05$) (Fig. 1). To determine if these findings depended on the choice of atlas, we performed the same analysis using the Harvard-Oxford atlas. Results using the Harvard-Oxford atlas were similar and are provided in Supplemental materials (A-1: Effects of Atlases, Fig. A1). To ensure that the distance measures were not affected by differences in brain volumes, we compared brain volumes between groups and found no statistical differences (Table A2) between the two groups for total brain, gray and white matter volumes. This is consistent with our previous published work, which found differences in regional brain volumes but no difference in total brain volume or overall white or gray matter volumes. We therefore did not include these parameters as covariates in our analyses (A-2: Comparisons of brain volumetric measures).

With the identified significant connections unique to the opioid-exposed group, we further determined the potential associations between the individual connection strengths and the highest Finnegan scores of the opioid-exposed subjects. Fig. 2 and Table 3 show the

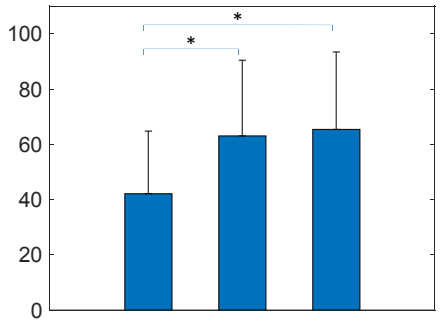

Comparison	T	P
Common vs unique opioid	-8.63	1.11E-16
Common vs unique controls	-9.88	0
Unique opioid vs unique controls	-0.66	0.5107

Fig. 1. Comparison of length of positive connections common to both groups, positive connections unique to the opioid-exposed group, and positive connections unique to controls.

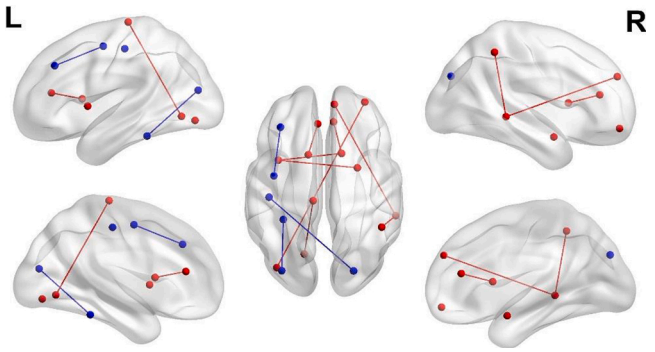

Fig. 2. Connections showing significant associations with highest Finnegan scores. Red lines and points represent a positive association with the highest Finnegan scores, while the blue lines and points represent negative association.

Table 3
Connections with significant associations with highest Finnegan scores.

Functional connection	R	p-value
L middle frontal gyrus – L precentral gyrus	−0.47	0.0431
L inferior occipital gyrus – R middle frontal gyrus, orbital part	0.54	0.0179
L middle temporal gyrus –R medial superior frontal gyrus	0.46	0.0462
R amygdala – L insula	0.67	0.0019
R caudate – L insula	0.55	0.0149
L caudate – L anterior cingulate gyrus	0.50	0.0304
R caudate – R anterior cingulate gyrus	0.68	0.0014
L Paracentral lobule – L lingual gyrus	0.55	0.0141
L postcentral gyrus – R superior occipital gyrus	−0.47	0.0437
L fusiform gyrus – L middle occipital gyrus	−0.50	0.0306
R middle temporal gyrus – R inferior parietal, supramarginal angular gyri	0.50	0.0291

connections exhibiting significant associations with the highest Finnegan scores (no correction for multiple comparisons). While these associations are marginally significant owing to the limited sample size, they are largely related to subcortical connections (4 out of 11), with the amygdala-insula connection and caudate-anterior cingulum connection among the smallest p-values, consistent with our previous findings showing reduced brain volumes in the subcortical areas in opioid-exposed infants (Merhar et al., 2020). Associations with the average Finnegan scores were also analyzed (A-4: Associations between connection strengths and Finnegan scores), exhibiting similar findings

(Figs. A5 and A6 and Table A4) as those using the highest Finnegan scores.

Rich-club coefficients with respect to a range of degrees (k) for both the opioid-exposed and control groups are shown in Fig. A7 for different sparsities. Both the opioid-exposed and control groups exhibit a rich-club topology span over a large range of k ($\Phi_{norm} > 1$). Although there appear to be some differences between the two groups for low sparsity, these were not statistically significant.

We evaluated in which known resting-state networks the unique and overlapping connections were seen and whether the connections were within the network (intra-network) or between networks (inter-network). As shown in Fig. 3, the connections unique to the opioid-exposed group were much more likely to be inter-network connections than the connections in the other two groups.

The distribution of betweenness centrality was different between the opioid-exposed group and controls (Fig. 4). Fig. 4a–c show the brain regions and Fig. 4d–f show the betweenness centrality distribution of the highest 25 % betweenness centrality for the opioid-exposed, controls, and overlapping connections, respectively. Regions with the highest betweenness centrality in the connections unique to the opioid-exposed group were the left inferior frontal gyrus (pars triangularis), left medial orbitofrontal cortex, right paracentral lobule, and left anterior cingulate cortex. In connections unique to the control group, these regions were the right inferior frontal gyrus (all subregions), the right precuneus, and the left superior medial frontal region. Betweenness centrality was overall higher in the regions among which connections overlapped between the two groups. Regions with highest betweenness centrality were bilateral insula, left anterior cingulate, right postcentral gyrus, left inferior orbitofrontal cortex, right middle cingulate, and the left superior occipital region.

3.2. Seed-based analysis

The seed-based network topologies of the opioid-exposed and controls in 8 networks – V1 (medial visual), V2 (occipital pole), V3 (lateral visual), DMN (default mode network), SM (sensorimotor), AN (auditory), SA (executive control/salience), FPN (bilateral frontoparietal), are shown in Fig. 5. We found no significant difference in individual strength between the two groups in any of these networks (Fig. 6a). However, the two groups showed different network topology. Controls had a larger number of connected voxels with all seed networks evaluated except for the default mode network (Fig. 6b). This is further illustrated by the dice index for each network. The dice index was <0.7 for all but one network (sensorimotor), suggesting that the opioid-exposed group and controls had different network topologies (Fig. 6c).

4. Discussion

The aim of this study was to investigate differences in functional networks and network-specific characteristics in infants with prenatal opioid exposure and controls. We found that connectivity and network topology are different in infants with prenatal opioid exposure. Specifically, we found different patterns of unique functional connections in each group, and different topologies and volumes of resting state networks. Our results suggest that prenatal opioid exposure influences brain connectivity early in life, which may underlie some of the later developmental, behavioral, and visual issues seen in this population.

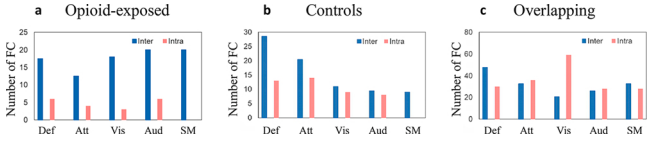

Fig. 3. Distribution of positive connections within networks. **a** Connections unique to opioid-exposed group **b** Connections unique to controls **c** Overlapping connections. Inter-network connections are shown in blue and intra-network connections are shown in red. Def = default mode, Att = attention, Vis = visual, Aud = auditory, SM = sensorimotor.

Our findings are consistent with previous work in neonates exposed to substances prenatally. Although the literature on infants exposed to opioids prenatally is sparse, opioids appear to affect brain volume (Merhar et al., 2020) and microstructure (Monnelly et al., 2018; Walhovd et al., 2012). In one small study of 10 opioid-exposed infants and 12 controls using seed-based analysis, higher resting-state connectivity between the right and left amygdala and several cortical regions were seen in the exposed group (Radhakrishnan et al., 2021). In the broader drug exposure literature, prenatal substance exposure has been associated with altered connectivity. Prenatal marijuana exposure is associated with hypoconnectivity in the insula and connections in the striatum (Grewen et al., 2015). Multi-drug exposure is associated with hyperconnectivity of the left amygdala to orbitofrontal cortex and hypoconnectivity of the posterior thalamus to the hippocampus (Grewen et al., 2015). Prenatal cocaine exposure is associated with hyperconnectivity between the thalamus and frontal regions, and polysubstance exposure is associated with hypoconnectivity between the thalamus and motor-related regions (Salzwedel et al., 2016). Prenatal substance exposure is associated with connectivity disruptions (both hyper- and hypo-connectivity) within the amygdala-frontal, insula--frontal, and insula-sensorimotor circuits (Salzwedel et al., 2015).

Opioid receptors are present in all areas of the brain, but especially widely distributed in the cortex, limbic system, and brain stem (Le Merrer et al., 2009). In experimental models, prenatal exposure to buprenorphine or methadone affects neurotransmitter biosynthesis (Wu et al., 2001), neurogenesis (Wu et al., 2014), and myelination (Vestal-Laborde et al., 2014; Sanchez et al., 2008). Prenatal opioid exposure induces long-term alterations in brain and behavior in rats, affecting multiple brain sites and multiple neurotransmitter systems (Vathy, 2002). Although the preclinical literature is inconsistent, likely due to different animal species and variations in type and dosing of opioids, it appears that prenatal opioid exposure alters normal modulatory influences in the developmental program of the brain in animal models (Malanga and Kosofsky, 1999).

Using a whole-brain connectomic approach, we found a unique pattern of connections in the opioid-exposed group and controls, with connections that were common to both groups. We evaluated betweenness centrality of nodes for overlapped connections and connections unique to each group. Nodes with high betweenness centrality are important for efficient communication across the network as a whole (Medaglia, 2017). Higher betweenness centrality means more connections through that node to achieve the shortest path lengths. The regions with the highest betweenness centrality we found that were unique to the opioid-exposed group included a number of nodes in the frontal, central and occipital regions, consistent with previously reported results (Gupta et al., 2012; Gill et al., 2003; Nelson et al., 1987; McGlone et al., 2014). It should be noted that there are different approaches to discerning brain functional hubs and brain hubs may vary depending on the approach by which hubs are defined (Rubinov and Sporns, 2010). We did not find a difference in rich-club coefficients between groups.

The connections unique to the opioid-exposed group were more often inter-network connections, while the connections that were unique to controls and those that overlapped were fairly evenly distributed between inter- and intra-network connections. Previous literature has shown that in networks that serve basic brain functions (auditory, visual, sensorimotor), intra-network connections increase with age, to increase functional specialization of those networks (Gao et al., 2015). In the higher order networks, inter-network connections increase with age, due to the multimodal nature of these higher order functions (Bertolero et al., 2017, 2015; Fair et al., 2009). Infants with prenatal opioid exposure who are experiencing withdrawal symptoms tend to be "disorganized" soon after birth and need decreased auditory and visual stimulation. We hypothesize that the increased inter-network

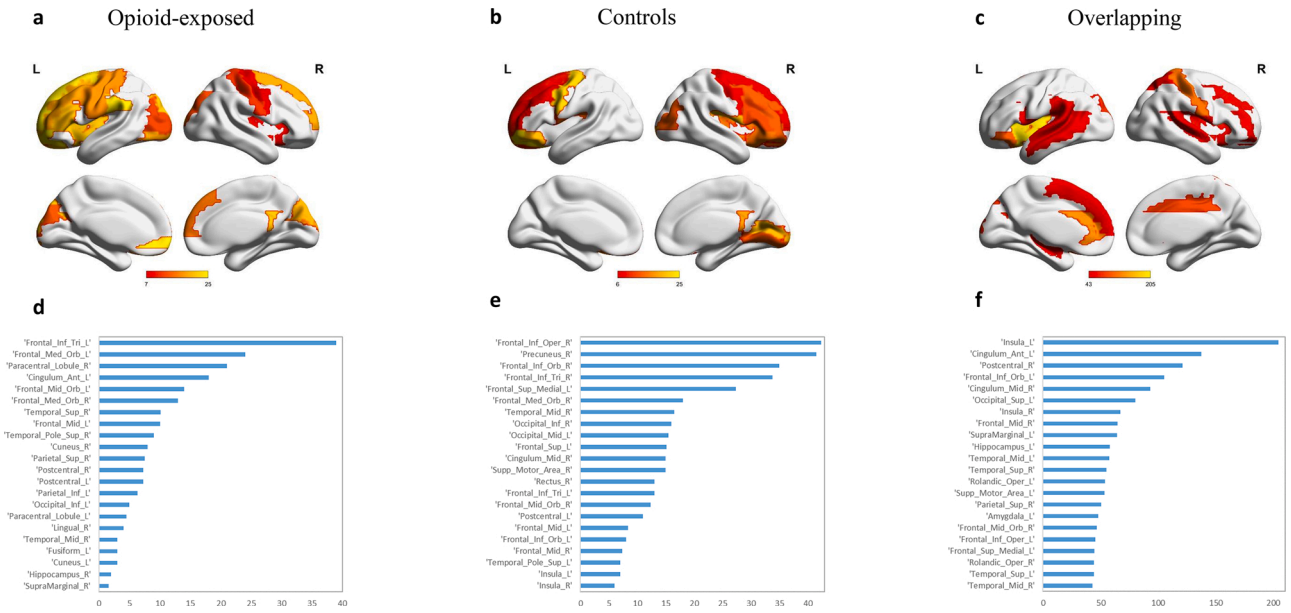

Fig. 4. Distribution of node betweenness centrality. **a** Betweenness centrality of unique positive connections in opioid-exposed group **b** Betweenness centrality of unique positive connections in controls **c** Distribution of betweenness centrality of overlapping connections seen in both groups **d** List of regions with the highest betweenness centrality unique to the opioid-exposed group **e** List of regions with the highest betweenness centrality unique to controls **f** List of regions with the highest betweenness centrality seen in both groups.

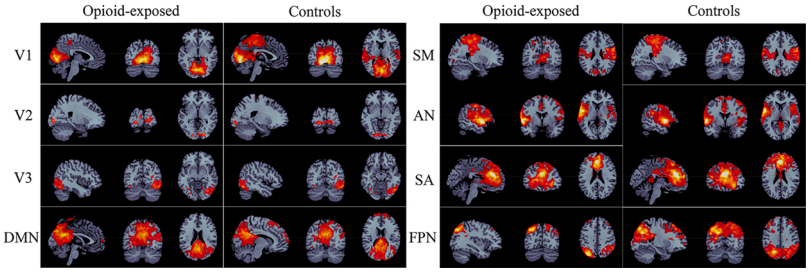

Fig. 5. Illustration of different network topologies in the opioid-exposed group versus controls. V1 = medial visual, V2 = occipital pole, V3 = lateral visual, DMN = default mode network, SM = sensorimotor, AN = auditory, SA = executive control/salience, FPN = bilateral frontoparietal.

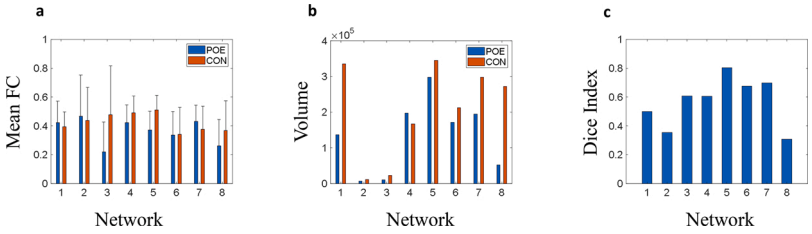

Fig. 6. Network strength and topology in opioid-exposed (blue) and control (red) groups. **a** Mean functional connectivity strength **b** Volume **c** Dice index. Network 1 = medial visual, Network 2 = occipital pole, Network 3 = lateral visual, Network 4 = default mode network, Network 5 = sensorimotor, Network 6 = auditory, Network 7 = executive control/salience, Network 8 = bilateral frontoparietal. FC = functional connectivity.

connections we see in the connections unique to this group, even in the basic sensory networks, reflect this outward disorganization. We found that the highest Finnegan score (a measure of withdrawal) was in fact correlated with connectivity, especially with those among subcortical brain regions, although the association did not survive correction for multiple comparisons. Further work is needed to investigate the relationship between differences in network organization and behavior.

The connections that were unique to the opioid-exposed group and the connections unique to controls were longer than those that overlapped between groups. Connection length tends to increase with age and myelination (Gao et al., 2011). Perinatal opioid exposure is known to adversely impact neurogenesis, programmed neuronal death, and myelination in murine models. Therefore, we hypothesize that the long-distance and inter-network connections are more vulnerable to prenatal opioid exposure, leading to differences between the groups.

Using seed-based analysis, we found that although mean functional connectivity strengths over the networks evaluated were not different between the opioid-exposed and control groups, the network volumes and topologies were different in most networks. The difference between network volumes and topology was particularly striking in the V1 network, with opioid-exposed children having markedly decreased network volume compared to controls. Children with prenatal opioid

exposure are known to have a higher risk of visual problems, including reduced visual acuity, strabismus, and nystagmus (Gupta et al., 2012; Gill et al., 2003; Nelson et al., 1987; McGlone et al., 2014). After prenatal exposure to methadone, infants show abnormal, smaller, or slower visual evoked potentials relative to controls (McGlone et al., 2008). Vision is a key function for later cognitive and behavioral development and may provide an early measure of brain functional integrity (Braddick and Atkinson, 2011). Although the neural substrate for the visual abnormalities seen with prenatal opioid exposure is unknown, opioid receptors are present in the cortex, in the lateral geniculate nucleus in the thalamus (visual relay center), and midbrain (responsible for some aspects of eye movements) (Walker et al., 1988). Our findings suggest that differences in the primary visual network could also potentially explain visual problems in children with prenatal opioid exposure.

Strengths of our study include rigorous imaging at a defined early time point. Groups were well-defined with results of maternal urine toxicology at the time of delivery for both opioid-exposed newborns and controls, and umbilical cord or meconium toxicology screens for all opioid-exposed infants. We were able to assess a brain-behavior connection by correlating Finnegan scores with connectivity.

Several limitations of our study should be considered. First, the sample size was small, and results should be validated in studies with larger sample sizes. We were unable to control for confounders including maternal smoking, maternal Hepatitis C, and maternal education, all of which have potential effects on brain development (Bublitz and Stroud, 2012; Salemi et al., 2014; Knickmeyer et al., 2017). Due to the small sample size, it was not possible to directly compare infants exposed to opioids *in utero* with and without these additional risk factors. This will be important in future studies. We chose to focus our analyses on positive connectivity, which may be seen as a limitation. To address this, we conducted additional analyses where absolute correlation coefficients were used, with results provided in the Supporting materials (A-3: Positive vs absolute correlation coefficients). Finally, although we are following this cohort to 2 years of age, in this study we were unable to evaluate neurodevelopmental outcomes.

5. Conclusions

Prenatal opioid exposure disrupts the architecture of brain networks. Future research using larger sample sizes and a longitudinal design, such as the upcoming HEALthy Brain and Child Development study, are required to understand how the type, timing, and duration of opioid exposure, as well as other confounding factors, affect the developing brain and subsequent neurodevelopment.

Funding

This work was supported by National Institutes of Drug Abuse (NIDA), part of NIH via R34 DA050268 (SM, JN, BK, JT) and R34 DA 050262 (WL).

Data statement

The datasets generated during the current study are available from the corresponding author on reasonable request.

CRediT authorship contribution statement

Stephanie L. Merhar: Conceptualization, Investigation, Funding acquisition, Project administration, Writing - original draft. **Weixiong Jiang:** Methodology, Visualization, Writing - review & editing. **Nehal A. Parikh:** Methodology, Resources, Supervision, Writing - review & editing. **Weiyan Yin:** Methodology, Writing - review & editing. **Zhen Zhou:** Formal analysis, Writing - review & editing. **Jean A. Tkach:** Data curation, Investigation, Methodology, Writing - review & editing. **Li Wang:** Methodology, Writing - review & editing. **Beth M. Kline-Fath:** Investigation, Methodology, Writing - review & editing. **Lili He:** Data curation, Funding acquisition, Writing - review & editing. **Adebayo Braimah:** Data curation, Formal analysis, Writing - review & editing. **Jennifer Vannest:** Conceptualization, Funding acquisition, Writing - original draft. **Weili Lin:** Conceptualization, Funding acquisition, Methodology, Supervision, Writing - review & editing.

Declaration of Competing Interest

The authors declare that they have no known competing financial interests or personal relationships that could have appeared to influence the work reported in this paper.

Acknowledgements

We would like to thank the participants and their families for their participation in the study and the research coordinators and MRI techs for their assistance with recruitment and scanning. We are grateful to Dr. Maria Barnes-Davis for her helpful comments that improved the manuscript.

Appendix A. Supplementary data

Supplementary material related to this article can be found, in the online version, at doi:https://doi.org/10.1016/j.dcn.2021.100996.

References

Alipio, J.B., Brockett, A.T., Fox, M.E., Tennyson, S.S., deBettencourt, C.A., El-Metwally, D., et al., 2020. Enduring consequences of perinatal fentanyl exposure in mice. Addict. Biol., e12895

Andersen, J.M., Høiseth, G., Nygaard, E., 2020. Prenatal exposure to methadone or buprenorphine and long-term outcomes: a meta-analysis. Early Hum. Dev. 143, 104997.

Arter, S.J., Tyler, B., McAllister, J., Kiel, E., Güler, A., Cameron Hay, M., 2021. Longitudinal outcomes of children exposed to opioids in-utero: a systematic review. J. Nurs. Scholarsh. 53 (1), 55–64. https://doi.org/10.1111/jnu.12609. Epub 2020 Nov 22.

Avants, B.B., Tustison, N.J., Song, G., Cook, P.A., Klein, A., Gee, J.C., 2011. A reproducible evaluation of ANTs similarity metric performance in brain image registration. Neuroimage 54, 2033–2044.

Badhwar, A., Collin-Verreault, Y., Orban, P., Urchs, S., Chouinard, I., Vogel, J., et al., 2020. Multivariate consistency of resting-state fMRI connectivity maps acquired on a single individual over 2.5 years, 13 sites and 3 vendors. Neuroimage 205, 116210.

Bertolero, M.A., Yeo, B.T., D'Esposito, M., 2015. The modular and integrative functional architecture of the human brain. Proc. Natl. Acad. Sci. U. S. A. 112, E6798–807.

Bertolero, M.A., Yeo, B.T.T., D'Esposito, M., 2017. The diverse club. Nat. Commun. 8, 1277.

Braddick, O., Atkinson, J., 2011. Development of human visual function. Vision Res. 51, 1588–1609.

Bublitz, M.H., Stroud, L.R., 2012. Maternal smoking during pregnancy and offspring brain structure and function: review and agenda for future research. Nicotine Tob. Res. 14, 388–397.

Chen, H.H., Chiang, Y.C., Yuan, Z.F., Kuo, C.C., Lai, M.D., Hung, T.W., et al., 2015. Buprenorphine, methadone, and morphine treatment during pregnancy: behavioral effects on the offspring in rats. Neuropsychiatr. Dis. Treat. 11, 609–618.

Erbs, E., Faget, L., Ceredig, R.A., Matifas, A., Vonesch, J.L., Kieffer, B.L., et al., 2016. Impact of chronic morphine on delta opioid receptor-expressing neurons in the mouse hippocampus. Neuroscience 313, 46–56.

Fair, D.A., Cohen, A.L., Power, J.D., Dosenbach, N.U., Church, J.A., Miezin, F.M., et al., 2009. Functional brain networks develop from a "local to distributed" organization. PLoS Comput. Biol. 5, e1000381.

Gao, W., Gilmore, J.H., Giovanello, K.S., Smith, J.K., Shen, D., Zhu, H., et al., 2011. Temporal and spatial evolution of brain network topology during the first two years of life. PLoS One 6, e25278.

Gao, W., Alcauter, S., Elton, A., Hernandez-Castillo, C.R., Smith, J.K., Ramirez, J., et al., 2015. Functional network development during the first year: relative sequence and socioeconomic correlations. Cereb. Cortex 25, 2919–2928.

Garrison, K.A., Scheinost, D., Finn, E.S., Shen, X., Constable, R.T., 2015. The (in)stability of functional brain network measures across thresholds. Neuroimage 118, 651–661.

Gill, A.C., Oei, J., Lewis, N.L., Younan, N., Kennedy, I., Lui, K., 2003. Strabismus in infants of opiate-dependent mothers. Acta Paediatr. 92, 379–385.

Grewen, K., Salzwedel, A.P., Gao, W., 2015. Functional connectivity disruption in neonates with prenatal marijuana exposure. Front. Hum. Neurosci. 9, 601.

Guo, H.Z., Enters, E.K., McDowell, K.P., Robinson, S.E., 1990. The effect of prenatal exposure to methadone on neurotransmitters in neonatal rats. Brain Res. Dev. Brain Res. 57, 296–298.

Gupta, M., Mulvihill, A.O., Lascaratos, G., Fleck, B.W., George, N.D., 2012. Nystagmus and reduced visual acuity secondary to drug exposure in utero: long-term follow-up. J. Pediatr. Ophthalmol. Strabismus 49, 58–63.
Holmes, C.J., Hoge, R., Collins, L., Woods, R., Toga, A.W., Evans, A.C., 1998. Enhancement of MR images using registration for signal averaging. J. Comput. Assist. Tomogr. 22, 324–333.
Honein, M.A., Boyle, C., Redfield, R.R., 2019. Public health surveillance of prenatal opioid exposure in mothers and infants. Pediatrics 143.
Hu, S., Sheng, W.S., Lokensgard, J.R., Peterson, P.K., 2002. Morphine induces apoptosis of human microglia and neurons. Neuropharmacology 42, 829–836.
Hutchison, R.M., Womelsdorf, T., Allen, E.A., Bandettini, P.A., Calhoun, V.D., Corbetta, M., et al., 2013. Dynamic functional connectivity: promise, issues, and interpretations. Neuroimage 80, 360–378.
Jiang, W., Zhang, H., Hsu, L.-M., Hu, D., Li, G., Wu, Y., et al., 2019a. Early development of infant brain complex network. In: Springer NatureMedical Image Computing and Computer Assisted Intervention – MICCAI 2019 MICCAI 2019 Lecture Notes in Computer Science, vol. 11765.
Jiang, W., Zhang, H., Hsu, L.-M., Hu, D., Li, G., Wu, Y., et al., 2019b. Early development of infant brain complex network. In: International Conference on Medical Image Computing and Computer-Assisted Intervention. Springer, pp. 832–840.
Juneja, P., Evans, P.M., Harris, E.J., 2013. The validation index: a new metric for validation of segmentation algorithms using two or more expert outlines with application to radiotherapy planning. IEEE Trans. Med. Imaging 32, 1481–1489.
Kam, T.-E., Wen, X., Jin, B., Jiao, Z., Hsu, L.-M., Zhou, Z., et al., 2019. A deep learning framework for noise component detection from resting-state functional MRI. Med. Image Comput. Comput. Assist. Interv. 754–762.
Knickmeyer, R.C., Xia, K., Lu, Z., Ahn, M., Jha, S.C., Zou, F., et al., 2017. Impact of demographic and obstetric factors on infant brain volumes: a population neuroscience study. Cereb. Cortex 27, 5616–5625.
Le Merrer, J., Becker, J.A., Befort, K., Kieffer, B.L., 2009. Reward processing by the opioid system in the brain. Physiol. Rev. 89, 1379–1412.
Lee, S.J., Bora, S., Austin, N.C., Westerman, A., Henderson, J.M.T., 2020. Neurodevelopmental outcomes of children born to opioid-dependent mothers: a systematic review and meta-analysis. Acad. Pediatr. 20, 308–318.
Malanga, C.J., Kosofsky, B.E., 1999. Mechanisms of action of drugs of abuse on the developing fetal brain. Clin. Perinatol. 26, 17–37 v-vi.
McGlone, L., Mactier, H., Hamilton, R., Bradnam, M.S., Boulton, R., Borland, W., et al., 2008. Visual evoked potentials in infants exposed to methadone in utero. Arch. Dis. Child. 93, 784–786.
McGlone, L., Hamilton, R., McCulloch, D.L., MacKinnon, J.R., Bradnam, M., Mactier, H., 2014. Visual outcome in infants born to drug-misusing mothers prescribed methadone in pregnancy. Br. J. Ophthalmol. 98, 238–245.
Medaglia, J.D., 2017. Graph theoretic analysis of resting state functional MR imaging. Neuroimaging Clin. N. Am. 27, 593–607.
Merhar, S.L., Kline, J.E., Braimah, A., Kline-Fath, B.M., Tkach, J.A., Altaye, M., et al., 2020. Prenatal opioid exposure is associated with smaller brain volumes in multiple regions. Pediatr. Res. https://doi.org/10.1038/s41390-020-01265-w. Online ahead of print.
Monnelly, V.J., Anblagan, D., Quigley, A., Cabez, M.B., Cooper, E.S., Mactier, H., et al., 2018. Prenatal methadone exposure is associated with altered neonatal brain development. Neuroimage Clin. 18, 9–14.
Monnelly, V.J., Hamilton, R., Chappell, F.M., Mactier, H., Boardman, J.P., 2019. Childhood neurodevelopment after prescription of maintenance methadone for opioid dependency in pregnancy: a systematic review and meta-analysis. Dev. Med. Child Neurol. 61, 750–760.
Nelson, L.B., Ehrlich, S., Calhoun, J.H., Matteucci, T., Finnegan, L.P., 1987. Occurrence of strabismus in infants born to drug-dependent women. Am. J. Dis. Child. 141, 175–178.
Nelson, L.F., Yocum, V.K., Patel, K.D., Qeadan, F., Hsi, A., Weitzen, S., 2020. Cognitive outcomes of young children after prenatal exposure to medications for opioid use disorder: a systematic review and meta-analysis. JAMA Netw. Open 3, e201195.
Radhakrishnan, R., Elsaid, N.M.H., Sadhasivam, S., Reher, T.A., Hines, A.C., Yoder, K.K., et al., 2021. Resting state functional MRI in infants with prenatal opioid exposure-a pilot study. Neuroradiology 63 (4), 585–591.
Robinson, S.E., Maher, J.R., Wallace, M.J., Kunko, P.M., 1997. Perinatal methadone exposure affects dopamine, norepinephrine, and serotonin in the weanling rat. Neurotoxicol. Teratol. 19, 295–303.
Roos, A., Fouche, J.P., Ipser, J.C., Narr, K.L., Woods, R.P., Zar, H.J., et al., 2021. Structural and functional brain network alterations in prenatal alcohol exposed neonates. Brain Imaging Behav. 15 (2), 689–699.
Rubinov, M., Sporns, O., 2010. Complex network measures of brain connectivity: uses and interpretations. Neuroimage 52, 1059–1069.
Salemi, J.L., Whiteman, V.E., August, E.M., Chandler, K., Mbah, A.K., Salihu, H.M., 2014. Maternal hepatitis B and hepatitis C infection and neonatal neurological outcomes. J. Viral Hepat. 21, e144–53.
Salzwedel, A.P., Grewen, K.M., Vachet, C., Gerig, G., Lin, W., Gao, W., 2015. Prenatal drug exposure affects neonatal brain functional connectivity. J. Neurosci. 35, 5860–5869.
Salzwedel, A.P., Grewen, K.M., Goldman, B.D., Gao, W., 2016. Thalamocortical functional connectivity and behavioral disruptions in neonates with prenatal cocaine exposure. Neurotoxicol. Teratol. 56, 16–25.
Sanchez, E.S., Bigbee, J.W., Fobbs, W., Robinson, S.E., Sato-Bigbee, C., 2008. Opioid addiction and pregnancy: perinatal exposure to buprenorphine affects myelination in the developing brain. Glia 56, 1017–1027.
Smith, S.M., Fox, P.T., Miller, K.L., Glahn, D.C., Fox, P.M., Mackay, C.E., et al., 2009. Correspondence of the brain's functional architecture during activation and rest. Proc. Natl. Acad. Sci. U. S. A. 106, 13040–13045.
Tao, H., Guo, S., Ge, T., Kendrick, K.M., Xue, Z., Liu, Z., et al., 2013. Depression uncouples brain hate circuit. Mol. Psychiatry 18, 101–111.
Tzourio-Mazoyer, N., Landeau, B., Papathanassiou, D., Crivello, F., Etard, O., Delcroix, N., et al., 2002. Automated anatomical labeling of activations in SPM using a macroscopic anatomical parcellation of the MNI MRI single-subject brain. Neuroimage 15, 273–289.
Van Dijk, K.R., Sabuncu, M.R., Buckner, R.L., 2012. The influence of head motion on intrinsic functional connectivity MRI. Neuroimage 59, 431–438.
Van Wagoner, S., Risser, J., Moyer, M., Lasky, D., 1980. Effect of maternally administered methadone on discrimination learning of rat offspring. Percept. Mot. Skills 50, 1119–1124.
Vathy, I., 2002. Prenatal opiate exposure: long-term CNS consequences in the stress system of the offspring. Psychoneuroendocrinology 27, 273–283.
Vestal-Laborde, A.A., Eschenroeder, A.C., Bigbee, J.W., Robinson, S.E., Sato-Bigbee, C., 2014. The opioid system and brain development: effects of methadone on the oligodendrocyte lineage and the early stages of myelination. Dev. Neurosci. 36, 409–421.
Walhovd, K.B., Watts, R., Amlien, I., Woodward, L.J., 2012. Neural tract development of infants born to methadone-maintained mothers. Pediatr. Neurol. 47, 1–6.
Walker, J.M., Bowen, W.D., Thompson, L.A., Frascella, J., Lehmkuhle, S., Hughes, H.C., 1988. Distribution of opiate receptors within visual structures of the cat brain. Exp. Brain Res. 73, 523–532.
Wang, L., Gao, Y., Shi, F., Li, G., Gilmore, J.H., Lin, W., et al., 2015. LINKS: learning-based multi-source IntegratioN frameworK for segmentation of infant brain images. Neuroimage 108, 160–172.
Wang, L., Li, G., Shi, F., Cao, X., Lian, C., Nie, D., et al., 2018. Volume-based analysis of 6-month-old infant brain MRI for autism biomarker identification and early diagnosis. Med. Image Comput. Comput. Assist. Interv. 11072, 411–419.
Weissenbacher, A., Kasess, C., Gerstl, F., Lanzenberger, R., Moser, E., Windischberger, C., 2009. Correlations and anticorrelations in resting-state functional connectivity MRI: a quantitative comparison of preprocessing strategies. Neuroimage 47, 1408–1416.
Wu, V.W., Mo, Q., Yabe, T., Schwartz, J.P., Robinson, S.E., 2001. Perinatal opioids reduce striatal nerve growth factor content in rat striatum. Eur. J. Pharmacol. 414, 211–214.
Wu, G., Wang, Q., Shen, D., 2012. Registration of longitudinal brain image sequences with implicit template and spatial-temporal heuristics. Neuroimage 59, 404–421.
Wu, C.C., Hung, C.J., Shen, C.H., Chen, W.Y., Chang, C.Y., Pan, H.C., et al., 2014. Prenatal buprenorphine exposure decreases neurogenesis in rats. Toxicol. Lett. 225, 92–101.
Yan, W., Zhang, H., Sui, J., Shen, D., 2018. Deep chronnectome learning via full bidirectional long short-term memory networks for MCI diagnosis. In: Medical Image Computing and Computer-Assisted Intervention: MICCAI International Conference on Medical Image Computing and Computer-Assisted Intervention, 11072, pp. 249–257.
Yan, W., Calhoun, V., Song, M., Cui, Y., Yan, H., Liu, S., et al., 2019. Discriminating schizophrenia using recurrent neural network applied on time courses of multi-site FMRI data. EBioMedicine 47, 543–552.
Yeoh, S.L., Eastwood, J., Wright, I.M., Morton, R., Melhuish, E., Ward, M., et al., 2019. Cognitive and motor outcomes of children with prenatal opioid exposure: a systematic review and meta-analysis. JAMA Netw. Open 2, e197025.
Zagon, I.S., McLaughlin, P.J., 1979. Motor activity and learning ability in rats perinatally exposed to methadone. NIDA Res. Monogr. 27, 121–127.
Zijdenbos, A.P., Dawant, B.M., Margolin, R.A., Palmer, A.C., 1994. Morphometric analysis of white matter lesions in MR images: method and validation. IEEE Trans. Med. Imaging 13, 716–724.